

Ignition delay times of methane and hydrogen highly diluted in carbon dioxide at high pressures up to 300 atm

Jiankun Shao^{a,*}, Rishav Choudhary^a, David F. Davidson^a,
Ronald K. Hanson^a, Samuel Barak^b, Subith Vasu^b

^a Department of Mechanical Engineering, Stanford University, Bldg. 520, Room 222, Stanford, CA 94305, USA

^b Center for Advanced Turbomachinery and Energy Research (CATER), Mechanical & Aerospace Engineering, University of Central Florida, Orlando, FL, 32816, US

Received 21 November 2017; accepted 1 August 2018

Available online 17 August 2018

Abstract

The need for more efficient power cycles has attracted interest in super-critical CO₂ (sCO₂) cycles. However, the effects of high CO₂ dilution on auto-ignition at extremely high pressures has not been studied in depth. As part of the effort to understand oxy-fuel combustion with massive CO₂ dilution, we have measured shock tube ignition delay times (IDT) for methane/O₂/CO₂ mixtures and hydrogen/O₂/CO₂ mixtures using sidewall pressure and OH* emission near 306 nm. Ignition delay time was measured in two different facilities behind reflected shock waves over a range of temperatures, 1045–1578 K, in different pressures and mixture regimes, i.e., CH₄/O₂/CO₂ mixtures at 27–286 atm and H₂/O₂/CO₂ mixtures at 37–311 atm. The measured data were compared with the predictions of two recent kinetics models. Fair agreement was found between model and experiment over most of the operating conditions studied. For those conditions where kinetic models fail, the current ignition delay time measurements provide useful target data for development and validation of the mechanisms.

© 2018 The Combustion Institute. Published by Elsevier Inc. All rights reserved.

Keywords: Super critical CO₂; Ignition delay time; High pressure; Shock tube

1. Background and introduction

The US Department of Energy (DOE) forecasts a 29% increase in the total electricity demand growing from 3826 billion kWh in 2012 to 4954 billion kWh in 2040, much of which is expected to be met by natural gas [1]. Natural gas-fired gas turbines

are set to become a vital part of future power generation. These turbines, however, are increasingly serving as major sources of CO₂, NO_x and other pollutants. The need for reducing greenhouse gas emissions like CO₂ and pollutants like NO_x is driven by regulation [2,3]. One of the possible solutions is oxy-fuel combustion with high CO₂ dilution so that the combustion products can be reduced mainly to CO₂ and H₂O, which can be recirculated into the feed. These advantages provide an opportunity for making high CO₂ dilution oxy-fuel

* Corresponding author.

E-mail address: jkshao@stanford.edu (J. Shao).

combustion-based power cycles a strong candidate for the next generation of power cycles. [4,5].

When carried out with sCO_2 as the working fluid instead of air and steam, gas turbines have the potential of higher overall efficiency and a significant downsizing in equipment size because of the higher energy density of sCO_2 fluids [4]. Although the advantages of the sCO_2 cycle are evident, there are very few experimental studies on the advanced sCO_2 combustion turbine engine. The chemical kinetics of oxy-fuel combustion in a CO_2 -diluted environment has not been well understood. However, it has already been shown that the combustion reactions behave differently with variation in the proportion of nitrogen and carbon dioxide [6,7], owing to their variable participation in combustion reactions directly or as a third-body collision partner. High-pressure shock tube ignition delays have been and continue to be one of the key sources of data that are important to characterize the combustion properties of real fuels. As part of the effort to understand the chemistry of the gas mixture with excess CO_2 , the ignition delay times for methane/ O_2/CO_2 mixtures and hydrogen/ O_2/CO_2 mixtures at the sCO_2 gas-turbine-related operating conditions are required.

In addition, there is an increasing interest in refining detailed kinetics models for combustion at high pressures. The existing knowledge base of combustion kinetics in excess CO_2 covers only low pressures and low CO_2 concentrations and does not overlap with the operating conditions of sCO_2 turbines. One necessary step in extending this knowledge base is to measure auto-ignition delay times at high pressures, which can serve as important design parameters for sCO_2 turbine cycles.

Most literature studies for methane and hydrogen ignitions are with low CO_2 concentrations ($< \sim 20\%$) [8–14]. Little work on high CO_2 concentration IDT measurements is available in the literature. Recently, Koroglu, et al. (2016) [7] conducted measurements for mixtures of CH_4 , CO_2 and O_2 in Argon bath gas at temperatures of 1577–2144 K, pressures of 0.53–4.4 atm, equivalence ratios of 0.5, 1, and 2, and CO_2 mole fractions of 0, 30, and 60%. Sensitivity analysis was carried out to identify critical reactions using the ARAMCO v2.0 mechanism. Three different influences in regard to chemistry, collision efficiencies, and heat capacities were examined as a result of CO_2 addition into the gas mixtures. The chemistry and global collision efficiency effects were found to be negligibly small to alter the IDT of methane for the experimental conditions of interest. More aggressive CO_2 addition was studied by Pryor et al. [15]; these authors conducted IDT experiments behind reflected shock waves at pressures between 0.6 and 1.2 atm, temperatures between 1650 and 2040 K, and an equivalence ratio equal to 1 for methane with CO_2 mole fraction varied between 0.0% to 89.5%. CH_4 concentrations were determined using an IR diode laser centered

at 3403.4 nm, and camera imaging was also used to account for shock bifurcation effects. The only high-pressure study for CO_2 rich mixtures was also reported by Pryor et al. [16]. The experiments were performed between 1300 K and 2000 K at pressures between 6 and 31 atm. The test mixtures were at an equivalence ratio of 1 with CH_4 mole fractions ranging from 3.5% to 5% and up to 85% CO_2 with a bath of Argon gas. Other work for CO_2 -rich mixtures is mainly focused on flame properties, such as laminar flame speed [17], burning rates [18], and flammability [19]. IDT data at higher pressures and increased CO_2 dilution is lacking.

In the current study, we have extended earlier studies to significantly higher pressures (27–311 atm), higher CO_2 concentration (above 85%) and to H_2 mixtures. We report the first high-pressure IDT measurements of methane and hydrogen, highly diluted in CO_2 for pressures up to 300 atm. Within the framework, we have also performed sensitivity analyses to understand the sub-mechanism that are expected to control the ignition process.

2. Experimental methods

Ignition delay times for the oxidation of hydrogen and methane were measured at near-stoichiometric conditions with various levels of CO_2 dilution. Pressure ranges examined spanned the range of $P_5 = 27\text{--}311$ atm, where P_5 is the reflected-shock pressure. The mixture compositions, as well as the facility used for each mixture, are shown in Table 1. The shock tube (ST) experiments were carried out in the high-pressure shock tubes at Stanford University (SU) and University of Central Florida (UCF). Both shock tubes have been well validated in former studies. The current test region is close to the operating conditions of a real sCO_2 turbine, majority of the tested conditions are above the vapor dome of CO_2 , i.e. they are in the supercritical region.

2.1. Stanford high-pressure shock tube and diagnostics

Current IDT experiments for all tests above 72 atm (test mixture 2, 4, and 6 in Table 1) were performed using the Stanford high-purity, high-pressure shock tube (HPST). The stainless steel driven section has an internal diameter of 5 cm and was heated to 363 K. Diaphragms were made of aluminum or steel (with cross-scribing of different depths) to allow measurements over a broad range of pressure (10–500 atm). In this shock tube, standard uniform test times (for non-reactive synthetic air mixtures) are of the order of 2 ms when helium is used as the driver gas. In current high CO_2 concentration experiments, the bifurcation effect, which is a non-ideal effect caused by boundary layer build-up [13], is stronger and the test times for

Table 1
IDT test conditions and facilities.

Mixture	Reactant mole fractions				Initial conditions		Facility
	CH ₄	H ₂	O ₂	CO ₂	T/K	P/atm	
1	0.075	0	0.15	0.775	1346–1434	27–35	UCF ST
2	0.075	0	0.15	0.775	1045–1411	100–286	SU HPST
3	0.0391	0	0.0992	0.8617	1447–1578	28–36	UCF ST
4	0.0391	0	0.0992	0.8617	1082–1453	72–269	SU HPST
5	0	0.05	0.1	0.85	1170–1270	37–40	UCF ST
6	0	0.1	0.05	0.85	1083–1291	103–311	SU HPST

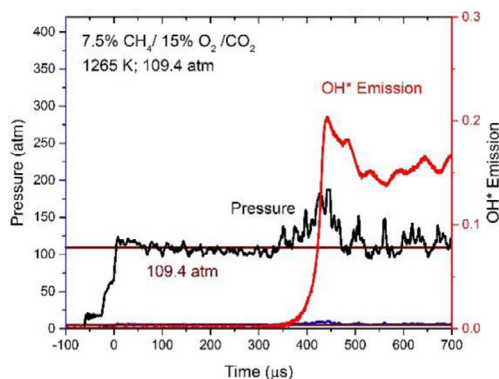


Fig 1. An example ignition delay time measurement for 7.5%CH₄/15%O₂/CO₂ mixture.

the current experiments are shorter, about 1.1 ms. High-purity methane, hydrogen, oxygen, and carbon dioxide gases were supplied by Praxair. Gas-phase fuel mixtures were prepared manometrically in a 12.8-liter stainless-steel mixing tank at 383 K. Mixtures were stirred using a magnetically-driven vane assembly for at least 15 minutes before the experiments.

Two diagnostics were employed during the experiments: excited OH radical (OH*) emission and sidewall PZT pressure; diagnostics in the HPST were located 1.1 cm away from the end wall. Ignition was indicated by emission near 306 nm from the A²Σ⁺ - X²Π ((0,0) band) of OH* that was detected using a modified PDA36A Si detector and Schott UG5 filter. Pressure time-histories are also monitored using a KistlerTM piezoelectric pressure transducer. With high CO₂ dilution in the test conditions, the pressure rise during ignition is not strongly obvious in most of the cases.

Example ignition data from the shock tube are shown in Fig 1; data include pressure traces and the OH* emission records. The IDT is defined as the time interval between the arrival of the reflected shock and the onset of ignition determined by extrapolating the maximum slope of OH* signals back to the baseline. In some cases, there is a pressure rise when ignition happens, and the IDTs defined by OH* emission and pressure trace are

consistent with each other. For most of the cases, the pressure does not change significantly when ignition occurs, and the IDT is defined using the OH* emission signal.

2.2. University of Central Florida (UCF) Shock tube and diagnostics

Current IDT experiments for all tests below 40 atm (test mixture 1, 3, 5 in Table 1) were performed using the large diameter (ID = 14 cm), heated, double-diaphragm UCF Shock Tube. For the current experiments, driven and driver sections were separated by polycarbonate sheets with thicknesses between 30 and 80 mil (0.762 and 2.032 mm). A double diaphragm method was used with two diaphragms separated by 10.2 cm. The mixtures were made using high purity gases purchased from PraxairTM (≥ 99.999%). A 33 L mixing tank with a magnetic stirrer was used to prepare each mixture before experiments. Two MKSTM Baratron (Models E27D and 628D) were used to measure the pressure during mixture preparation. The mole fractions for each of the constituent compounds were determined using partial pressures. The pressure behind the reflected shock wave was measured using a KistlerTM 603B1 pressure transducer located 2 cm from the driven section end wall. Unfiltered emission was measured at the same location and the arrival of reflected shock wave was monitored using laser schlieren technique. [16]

Example ignition data are shown in Fig 2; data include pressure traces and the emission records. The IDT is defined as the time interval between the arrival of the reflected shock, which is defined as the time between laser schlieren peak and the onset of ignition determined by extrapolating the maximum slope of the emissions signal back to the baseline. Note, to avoid the uncertainty in time zero associated with the reflected shock bifurcation, laser schlieren peaks were used to accurately determine time zero.

2.3. Uncertainty and non-ideal effects

Temperatures and pressures in the current shock wave experiments are well-characterized by standard shock relations. The pressure time-histories are compared with calculated P₅ in Figs 1 and 2.

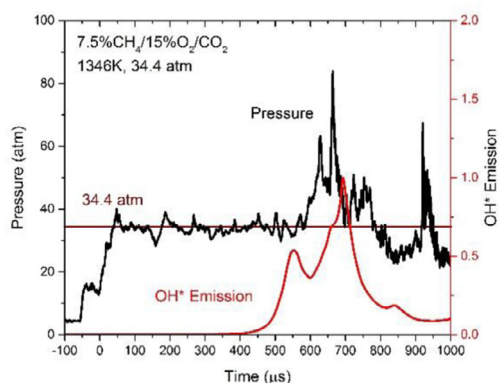


Fig 2. An example Ignition delay time measurement for 7.5%CH₄/15%O₂/CO₂ mixture.

Accurate measurements of the incident shock speed translate into accurate determinations of reflected shock temperatures and pressures. The shock arrival times in the driven section of the shock tube were recorded by five piezoelectric pressure transducers. The velocity of the incident shock at the end wall was then determined by extrapolation, allowing calculation of the initial reflected shock temperature and pressure, using one-dimensional shock-jump relations and assuming vibrational equilibrium and frozen chemistry, with resulting uncertainties in initial post-shock temperature and pressure of less than $\pm 1\%$.

The 2-Sigma uncertainty of individual ignition delay data points is $\pm 25\%$ and this value is used in the error bars in the accompanying figures. The uncertainty is estimated by the theory of propagation of uncertainty with the primary contribution being from the $\pm 1\%$ uncertainty in the initial reflected-shock temperature. Another main source of the uncertainty is dP_5^*/dt (where $dP_5^* = dP_5/P_5$). For the H₂/O₂/CO₂ mixture, the dP_5^*/dt is negligible. For the CH₄/O₂/CO₂ mixtures, the maximum dP_5^*/dt value for current studies is about $-0.1/\text{ms}$. The comparison of a constant pressure simulation and a specified pressure simulation at 1250 K is conducted for 7.5% CH₄/15% O₂/CO₂ mixture using Chemkin software package. The $-0.1/\text{ms}$ level dP_5^*/dt will lead to an about 5% shift in IDT values estimated from simulations. In addition, the OH* emission signal is weak at highly diluted condition, which contributes an additional 10% uncertainty on the IDT definition. For current studies, we included these into the 25% overall uncertainty. For future applications of mechanism validations, specified pressure simulations with measured pressure histories would be suggested. Other minor factors contribute overall uncertainties that are typically by order 1% including determination of the IDT interval based on the maximum slope criterion and

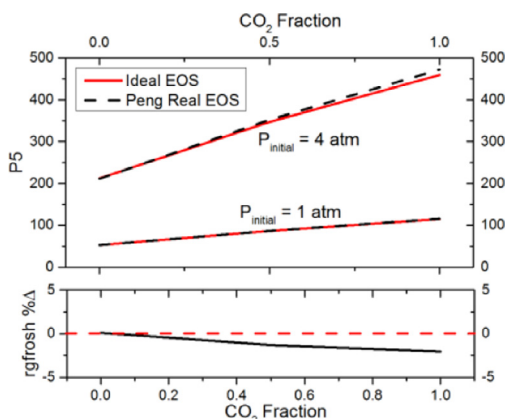


Fig 3. Comparison of real gas and ideal gas shock wave calculations of reflected shock pressure for CO₂/Ar mixtures; $\% \Delta = (P_{\text{realEOS}} - P_{\text{idealEOS}}) / P_{\text{idealEOS}}$.

the ideal equation of state used for test region calculations.

Use of the ideal CO₂ equation of state at these high pressures was validated by noting that the calculated and measured reflected shock pressures were in close agreement. As shown in Fig 3, the pressure after the reflected shock wave was calculated for initial pre-shock pressures of 1 atm and 4 atm with an incident shock wave speed of 1 mm/ μs , as a function of CO₂ mole fraction. A higher initial pressure yields a higher P_5 . Two separate equations of state are used in the calculations, the Peng–Robinson real gas equation of state and the ideal gas equation of state. The percentage pressure difference of the calculations using the two EOS is also shown on the bottom of Fig 3; the maximum difference is found to be 2% at 472 atm with pure CO₂. Thus, in the current study, the test region conditions are calculated using ideal EOS, and the calculated pressures are directly compared with measurements using a Kistler PZT pressure transducer.

At pressures and temperatures of importance to practical applications, concerns have recently been raised about the effect of shock wave bifurcation observed behind reflected shock waves using imaging techniques [15]. Bifurcation is the separation of the normal shock wave into two different oblique shockwaves inside the boundary layer [7,20,21]. This effect can cause some difficulty in the time zero definition. However, in most of the current test conditions, the pressure rise after reflected shock wave is very sharp, and a significant bifurcation was not evident. This is likely an outcome of the thinness of the boundary layer at high pressures. The core section of the post-shock region that comprises most of the flow area still has the gases at the calculated T_5 and P_5 , as discussed by Koroglu et al. (2016) [7]. In cases with an observable bifurcation in the pressure trace, an accurate

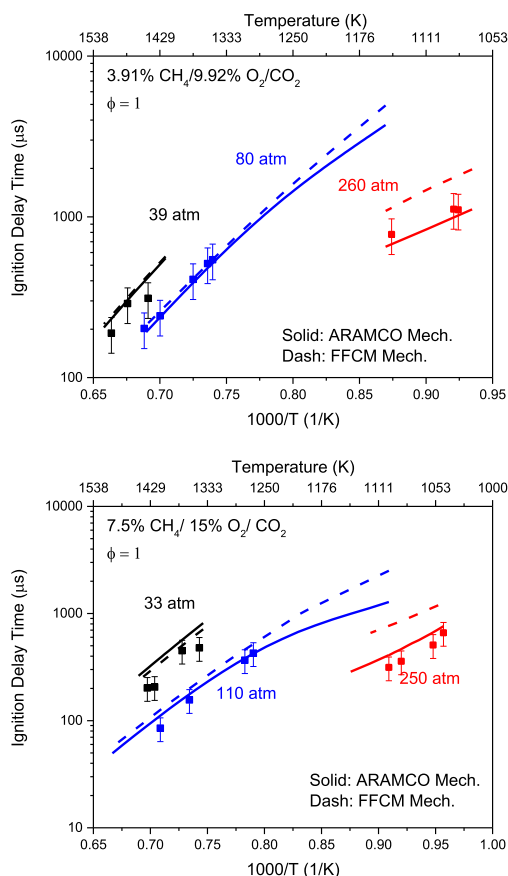


Fig 4. Ignition delay time measurement for $\text{CH}_4/\text{O}_2/\text{CO}_2$ mixtures.

time zero was determined using the beam-steering schlieren peak from IR diode laser beam (centered at 3403.4 nm) that transverses the shock tube at the test location.

3. Results and discussion

In this section, the IDT data of the current measurements for $\text{CH}_4/\text{O}_2/\text{CO}_2$ and $\text{H}_2/\text{O}_2/\text{CO}_2$ mixtures are reported. These are the first reported high-pressure, CH_4/H_2 highly diluted in CO_2 , IDT data to our knowledge. Tables of the test conditions and measured IDT values can be found in the supplementary material. Results are compared to two widely validated chemical mechanisms: ARAMCO v2.0 and FFCM (2018) [22,23].

3.1. $\text{CH}_4/\text{O}_2/\text{CO}_2$ mixtures

The measured IDTs for $\text{CH}_4/\text{O}_2/\text{CO}_2$ mixtures are plotted in Fig 4. IDT measurements were performed near 30 atm, 80 atm and 260 atm for the

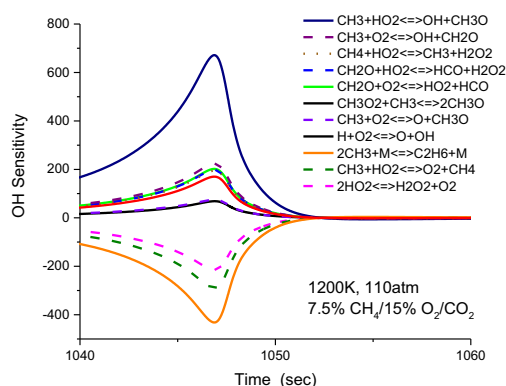


Fig 5. OH Sensitivity for high pressure methane ignition. Simulation using FFCM (2018) model showing top 11 sensitive reactions.

3.91% methane/9.92% oxygen/carbon dioxide mixture, and near 33 atm, 110 atm and 250 atm for the 7.5% methane/15% oxygen/carbon dioxide mixture.

In Fig 4, experimental results are compared to predictions of detailed mechanisms. At operating conditions lower than 110 atm, both mechanisms predict similar IDT values and match the measurements with a deviation less than 20%. At higher pressures, the discrepancy between the two kinetics mechanisms increases and the ARAMCO mechanism better predicts the IDT near 250 atm. On the other hand, it should be noted that even at 110 atm, the two mechanisms have different predictions when the temperature is lower than 1200 K for the 7.5% $\text{CH}_4/15\% \text{O}_2/\text{CO}_2$ mixture, supporting the need to extend the current work to lower temperatures. The present obstacle to doing this is extending the shock tube test time and dealing with the bifurcation and remote ignition that may occur. In previous studies, we have successfully extended shock tube test time to 50 + ms by adjusting driver gas [24] and have eliminated remote ignition and reduced boundary layer effects by using a constrained reactive volume strategy [25]. Future measurements at lower temperatures will implement these methods.

Figure 5 presents a detail (near 1070 μs) of the OH sensitivity analysis for one high pressure CH_4 ignition example using the FFCM (2018) model. The importance of the listed reactions and their behavior has not been carefully investigated at high pressures, and assumptions about the rate constants and reaction products are based on lower pressure (typically by a factor of 100) experiments and simulations. The OH radical pool, which is expected to have some control over the ignition timing, is primarily sensitive to a series of reactions of the two key species HO_2 and CH_3 , including several reactions that are expected to form stabilized

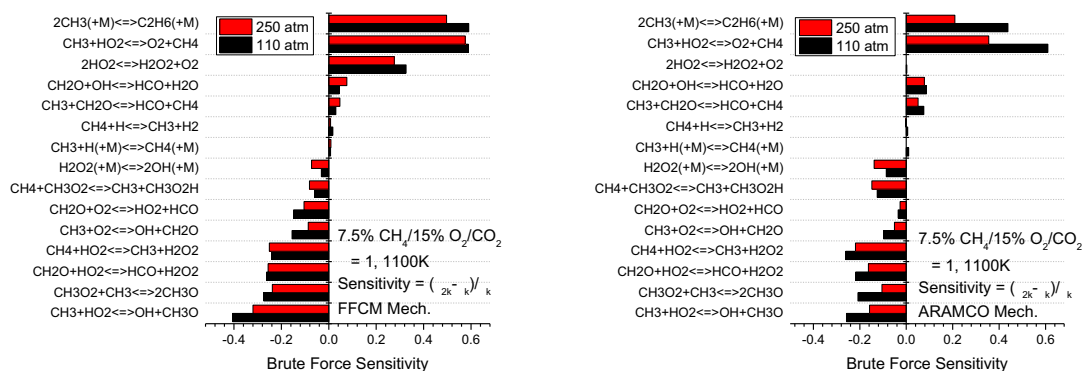


Fig 6. Brute force sensitivity of IDT at 1100 K using FFCM (2018) mechanism and ARAMCO mechanism.

intermediates at high pressures. Though the current models provide relatively good agreement with the measurements, two mechanisms show different sensitivities for some reactions.

Additional fundamental rate constant measurements are needed at high pressures to validate these results.

Figure 6 shows the brute force sensitivity of ignition delay time at 1100 K using FFCM (2018) mechanism and ARAMCO mechanism. Both mechanisms show some reactions with methyl radical play an important role, which confirms the necessity to study these reactions at high pressures. Figure 6 also shows there is an observable discrepancy between the two mechanisms. For example, $2\text{CH}_3(+\text{M}) \rightleftharpoons \text{C}_2\text{H}_6(+\text{M})$ reaction, which was identified as the most important reaction at 110 atm in FFCM (2018) mechanism, was not as important as $\text{CH}_3 + \text{HO}_2 \rightleftharpoons \text{O}_2 + \text{CH}_4$ in ARAMCO mechanism. In addition, $2\text{HO}_2 \rightleftharpoons \text{H}_2\text{O}_2 + \text{O}_2$ is identified to be an important reaction in FFCM (2018) mechanism, but it is not important in ARAMCO mechanism. Additional high-pressure reaction rate measurements are required to improve the predictions these auto-ignition phenomenon. Another observation is the dominant reactions will not change with pressure. ARAMCO mechanism shows the absolute sensitivity values might change with pressure, but the reactions that dominate the uncertainty analysis are unchanged at high pressures. This observation shows the pressure dependence may not be the only explanation of the discrepancy between the FFCM (2018) mechanism prediction and experiments at 250 atm. The discrepancy might also come from temperature dependence, note that lower pressure experiments were conducted at a higher temperatures.

Figure 7 shows the comparison of the temperature dependence of ignition delay time brute force sensitivity at 110 atm using two mechanisms. There are some observable discrepancies between the two mechanisms. However, there are also some consis-

tent predictions. For example, they both predicted the sensitivity of most reactions will decrease with temperature, except $\text{CH}_3 + \text{HO}_2 \rightleftharpoons \text{OH} + \text{CH}_3\text{O}$, $\text{CH}_3 + \text{O}_2 \rightleftharpoons \text{OH} + \text{CH}_2\text{O}$, and $\text{CH}_2\text{O} + \text{O}_2 \rightleftharpoons \text{HO}_2 + \text{HCO}$. In addition, FFCM (2018) mechanism works better at high temperatures, which implies the reactions having a large temperature dependence might contribute to the discrepancy, such as $\text{CH}_3\text{O}_2 + \text{CH}_3 \rightleftharpoons 2\text{CH}_3\text{O}$, $\text{CH}_2\text{O} + \text{HO}_2 \rightleftharpoons \text{HCO} + \text{H}_2\text{O}_2$, $\text{CH}_4 + \text{HO}_2 \rightleftharpoons \text{CH}_3 + \text{H}_2\text{O}_2$, $2\text{CH}_3(+\text{M}) \rightleftharpoons \text{C}_2\text{H}_6(+\text{M})$, $\text{CH}_3 + \text{HO}_2 \rightleftharpoons \text{O}_2 + \text{CH}_4$ and $2\text{HO}_2 \rightleftharpoons \text{H}_2\text{O}_2 + \text{O}_2$. Accurate high-pressure rate measurements for these reactions are required.

3.2. $\text{H}_2/\text{O}_2/\text{CO}_2$ mixtures

Figure 8 presents the current IDT measurements and simulations for $\text{H}_2/\text{O}_2/\text{CO}_2$ mixtures. IDT measurements for 10% $\text{H}_2/5\% \text{O}_2/\text{CO}_2$ mixtures were performed near 110 atm and 250 atm. IDT measurements for 5% $\text{H}_2/10\% \text{O}_2/\text{CO}_2$ mixture were performed near 40 atm. The upper plot of Fig 8 shows the high-pressure data (110 and 250 atm) from Stanford shock tube, and the lower plot shows the data near 39 atm from UCF shock tube.

Both mechanisms predict the current measurements within 20%. The current work confirms the capability of the hydrogen ignition prediction of the two mechanisms in the tested operating conditions. Activation energies for both the FFCM (2018) mechanism and the ARAMCO mechanism are effectively the same. Sensitivity analysis using the FFCM (2018) mechanism, shown in Fig 9 indicates that almost all the HO_2 and H_2O_2 reactions in the H_2/O_2 mechanism may play some role in controlling the H-atom, OH and HO_2 radical concentrations and thus the overall oxidation process. At the high pressures of these experiments, few of these reactions have been measured and the overall $\text{HO}_2/\text{H}_2\text{O}_2$ sub-mechanism has not been validated.

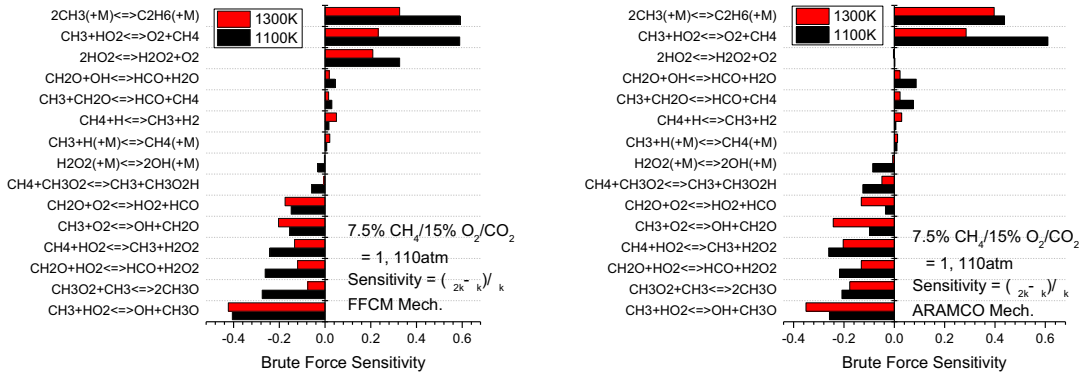


Fig 7. Brute force sensitivity of IDT at 110 atm using FFCM (2018) mechanism and ARAMCO mechanism.

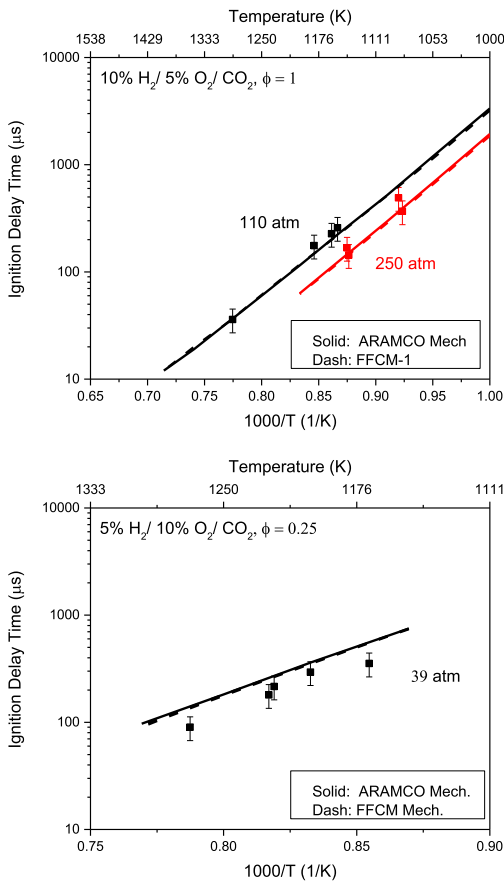


Fig 8. Ignition delay time measurement for $\text{H}_2/\text{O}_2/\text{CO}_2$ mixtures.

4. Conclusion

Ignition delay times of $\text{CH}_4/\text{O}_2/\text{CO}_2$ and $\text{H}_2/\text{O}_2/\text{CO}_2$ mixtures were studied in high-pressure

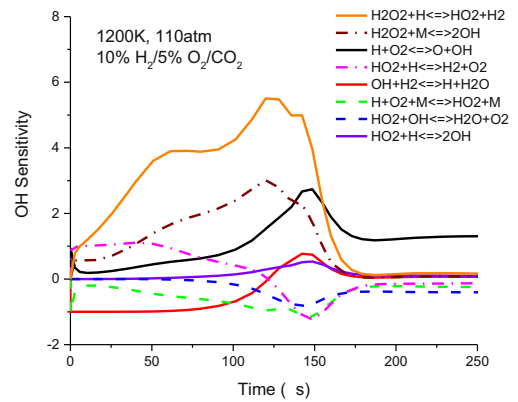


Fig 9. OH Sensitivity for high pressure hydrogen ignition. Simulation using FFCM (2018) model showing top 8 sensitive reactions.

shock tubes. IDT measurements were performed from 27 atm to 286 atm for methane/oxygen/carbon dioxide mixtures and from 37 atm to 311 atm for hydrogen/oxygen/carbon dioxide mixtures. The current experiments were the first methane/hydrogen highly diluted in CO_2 ignition delay time data at these elevated pressures, which are necessary data for future CO_2 -rich gas turbine engine design and also critical to validate and refine foundational kinetics mechanisms at these extreme conditions. Sensitivity analyses were conducted for both systems; there is a significant role of CH_3 kinetics in the methane system and of $\text{HO}_2/\text{H}_2\text{O}_2$ kinetics in both systems. These first experiments indicate that further high-pressure IDT and fundamental rate constant measurements in these systems are needed to increase confidence in the high pressure modeling of syngas mixtures.

Acknowledgments

This material is based upon work supported by the U.S. Department of Energy under Award Number DE-FE0025260. The authors thank Frank Barnes, Erik Ninnemann, and Sneha Neupane for assistance with UCF shock tube experiments.

Disclaimer

This report was prepared as an account of work sponsored by an agency of the United States Government. Neither the United States Government nor any agency thereof, nor any of their employees, makes any warranty, express or implied, or assumes any legal liability or responsibility for the accuracy, completeness, or usefulness of any information, apparatus, product, or process disclosed, or represents that its use would not infringe privately owned rights. Reference herein to any specific commercial product, process, or service by trade name, trademark, manufacturer, or otherwise does not necessarily constitute or imply its endorsement, recommendation, or favoring by the United States Government or any agency thereof. The views and opinions of authors expressed herein do not necessarily state or reflect those of the United States Government or any agency thereof.

Supplementary materials

Supplementary material associated with this article can be found, in the online version, at doi:[10.1016/j.proci.2018.08.002](https://doi.org/10.1016/j.proci.2018.08.002).

References

- DOE/EIA. Annual Energy Outlook 2014; Available from: <http://www.eia.gov/forecasts/aeo/pdf/0383.pdf>. (2014).
- M. Meinshausen, N. Meinshausen, W. Hare, S.C. Raper, K. Frieler, R. Knutti, M.R. Allen, *Nature* 458 (7242) (2009) 1158–1162.
- D.W. Stanton, *SAE Int. J. Engines* 6 (3) (2013) 1395–1480.
- V. Dostal, A supercritical carbon dioxide cycle for next-generation nuclear reactors, Doctoral dissertation, Massachusetts Institute of Technology, Department of Nuclear Engineering, 2004.
- R.J. Allam, J.E. Fetvedt, B.A. Forrest, D.A. Freed, *ASME Turbo Expo 2014: Turbine Technical Conference and Exposition*, 2014, June V03BT36A016–V03BT36A016 American Society of Mechanical Engineers.
- X. Hu, Q. Yu, J. Liu, N. Sun, *Energy* 70 (2014) 626–634.
- B. Koroglu, O.M. Pryor, J. Lopez, L. Nash, S.S. Vasu, *Combust. Flame* 164 (2016) 152–163.
- J. Shao, D.F. Davidson, R.K. Hanson, *Fuel* 225 (2018) 370–380.
- J. Shao, R. Choudhary, A. Susa, D.F. Davidson, R.K. Hanson, in: *Proceedings of the Combustion Institute*, 2018.
- J. Herzler, Y. Sakai, M. Fikri, C. Schulz, in: *Proceedings of the Combustion Institute*, 2018.
- A. Schneider, J. Mantzaras*, S. Eriksson, *Combust. Sci. Technol.* 180 (1) (2007) 89–126.
- P. Glarborg, L.L. Bentzen, *Energy Fuels* 22 (1) (2007) 291–296.
- T. Le Cong, & P. Dagaut. *Proc. Combust. Inst.*, 32(1), (2009) 427–435.
- F.L. Dryer, M. Chaos, *Combust. Flame* 152 (1,2) (2008) 293–299.
- O. Pryor, S. Barak, B. Koroglu, E. Ninnemann, S.S. Vasu, *Combust. Flame* 180 (2017) 63–76.
- O. Pryor, S. Barak, J. Lopez, E. Ninnemann, B. Koroglu, L. Nash, S.S. Vasu, *J. Energy Resources Technol.* 139 (4) (2017) 042208.
- B. Almansour, L. Thompson, J. Lopez, G. Barari, S.S. Vasu, *J. Energy Resources Technol.* 138 (3) (2016) 032201.
- P. Heil, D. Toporov, M. Förster, R. Kneer, *Proc. Combust. Inst* 33 (2) (2011) 3407–3413.
- A. Di Benedetto, F. Cammarota, V. Di Sarli, E. Salzano, G. Russo, *Chem. Eng. Sci* 84 (2012) 142–147.
- R.K. Hanson, & D.F. Davidson, *Prog. Energy Combust. Sci.*, 44, (2014) 103–114.
- V. Dostal, P. Hejzlar, M.J. Driscoll, *Nuclear Technol.* 154 (3) (2006) 283–301.
- W.K. Metcalfe, S.M. Burke, S.S. Ahmed, H.J. Curran, *Int. J. Chem. Kinetics* 45 (10) (2013) 638–675.
- G.P. Smith, Y. Tao, and H. Wang, *Foundational Fuel Chemistry Model Version 1.0 (FFCM-1)*, <http://nanoenergy.stanford.edu/ffcm1>, 2016.
- Z. Hong, G.A. Pang, S.S. Vasu, D.F. Davidson, R.K. Hanson, *Shock Waves* 19 (2) (2009) 113–123.
- R.K. Hanson, G.A. Pang, S. Chakraborty, W. Ren, S. Wang, D.F. Davidson, *Combust. Flame* 160 (9) (2013) 1550–1558.